

RESEARCH ARTICLE



A qualitative prognostic biomarker for melanoma based on the relative methylation orderings of CpG loci

Yue Huo^a, Yaru Gao^a, Jiayi Ruan^b, Lingli Wang^b, Hongdong Li^b, and Guini Hong ^b

^aSchool of Public Health and Health Management, Gannan Medical University, Ganzhou, China; ^bSchool of Medical Information Engineering, Gannan Medical University, Ganzhou, China

ABSTRACT

Skin cutaneous melanoma (SKCM) is an aggressive tumor with a poor prognosis. We developed SKCM-P8, a novel qualitative prognostic biomarker based on the relative methylation orderings of eight pairs of loci. Analysis of a training cohort and two independent validation datasets revealed a significant difference in overall survival between high- and low-risk groups stratified by SKCM-P8 ($p < 0.05$, log-rank test), with average area under the curve values of 0.83, 0.80, and 0.61, respectively. The differential methylation loci between high- and low-risk patients were enriched in immune-related biological processes and signaling pathways. Furthermore, low-risk patients exhibited higher CD8⁺ T cells and B levels, while high-risk patients had higher monocytes. The methylation levels of SKCM-P8 were also correlated with immune cell levels, indicating that they can reflect prognosis-related immune information. The low-risk group had a significantly higher mutation burden ($p < 0.05$, Wilcoxon test), suggesting potential benefits from immune checkpoint inhibitors. Patients stratified by SKCM-P8 displayed differential responses to therapy and immunotherapy ($p < 0.05$, Wilcoxon test), with low-risk patients showing better sensitivity and response. Furthermore, SKCM-P8 demonstrated super-predictive accuracy compared to six published models. Overall, SKCM-P8 offers a promising tool for predicting prognosis and guiding therapeutic decisions in SKCM.

ARTICLE HISTORY

Received 3 November 2024
Revised 6 March 2025
Accepted 26 March 2025




KEYWORDS

Melanoma; prognosis;
relative methylation
orderings

Introduction

Skin cutaneous melanoma (SKCM) is a malignant tumor characterized by high rates of invasiveness and metastasis. The 5-year survival rate for primary SKCM is as high as 95%, while it drops to less than 10% in metastatic SKCM patients [1]. Early detection and treatment can reduce the chances of metastasis and improve patients' cure and survival rates. However, in the clinic, the risk stratification and prognosis of SKCM patients mainly depend on clinicopathologic features such as Breslow thickness, ulceration, and microsatellite metastasis [2]. Due to the tumor heterogeneity, these conventional clinical features have limited effectiveness in accurately predicting individual patient outcomes and survival [3]. Therefore, it is essential to identify sensitive prognostic biomarkers that may have clinical applications.

DNA methylation is an important epigenetic process [4], and aberrant DNA methylation is closely associated with tumorigenesis and progression [5]. Several studies have demonstrated that DNA methylation patterns can be prognostic indicators for SKCM [6–8]. For example, Guo et al. identified four methylation loci significantly associated with SKCM prognosis by analyzing SKCM samples from The Cancer Genome Atlas (TCGA), demonstrating good predictive efficacy [9]. Li et al. classified SKCM patients into seven subtypes using cluster analysis, revealing significant prognostic differences among these subtypes [10]. Ralser et al. discovered two methylation loci (cg18561976, cg15344028) in the *ICOS* gene significantly associated with SKCM prognosis [11]. However, the prediction accuracy of these methylation loci typically relies on their quantitative

CONTACT Hongdong Li  biomantis_lhd@163.com; Guini Hong  hongguini08@gmail.com  School of Medical Information Engineering, Gannan Medical University, Huangjin Campus, University Town, Rongjiang New District, Ganzhou, Jiangxi 341000, China
 Supplemental data for this article can be accessed online at <https://doi.org/10.1080/15592294.2025.2487316>

© 2025 The Author(s). Published by Informa UK Limited, trading as Taylor & Francis Group.

This is an Open Access article distributed under the terms of the Creative Commons Attribution-NonCommercial License (<http://creativecommons.org/licenses/by-nc/4.0/>), which permits unrestricted non-commercial use, distribution, and reproduction in any medium, provided the original work is properly cited. The terms on which this article has been published allow the posting of the Accepted Manuscript in a repository by the author(s) or with their consent.

methylation levels measured in the training sets, which are susceptible to batch effects, restricting their validation in independent datasets, and limiting their clinical applications.

We previously proposed a novel method for identifying qualitative cancer diagnostic biomarkers by utilizing the within-sample relative methylation orderings (RMOs) of CpG loci pairs [12]. This approach addresses the issue of experimental batch effects commonly encountered in quantitative methylation-level measurements, improving the model's reliability across different datasets [13]. Building on this RMO approach, Ge et al. constructed a prognostic model containing 10 methylation loci pairs that accurately predicted the prognosis of patients with acute myeloid leukemia [14]. Similarly, Wei et al. developed a prognostic model comprising seven methylation loci pairs for clear cell renal cell carcinoma and demonstrated good predictive efficacy in the validation set [15]. These findings demonstrate the effectiveness of RMO-based qualitative biomarker for diagnosing and predicting outcomes for various cancer types.

Therefore, by focusing on the within-sample RMOs, which circumvent the limitations of biomarkers based on traditional quantitative methylation levels, we aim to identify a novel prognostic biomarker for SKCM that not only enhances prognostic accuracy but also facilitates personalized treatment strategies, ultimately improving patient outcomes in SKCM. This research has the potential to pioneer a more robust framework for integrating epigenetic data into clinical practice, marking a significant advance in the field of precision oncology.

Materials and methods

Data source and data preprocessing

The SKCM DNA methylation data and associated clinical information analyzed in this study were downloaded from the TCGA and Gene Expression Omnibus (GEO) databases, as outlined in Table 1.

Data were preprocessed using the R package ChAMP. First, we remove non-GpG methylation loci and SNP-related methylation loci. Then, we exclude loci mapped to multiple locations and those

Table 1. Datasets used in this study.

Dataset	Data type	Sample size	Platform
TCGA-SKCM	DNA methylation	458	Illumina 450k
	RNA sequencing	457	Illumina HiSeq 2000
	Somatic mutation	454	Illumina TSO500
GSE51547	DNA methylation	47	Illumina 450k
GSE144487	DNA methylation	194	Illumina 850k

on sex chromosomes. We also deleted loci with over 70% missing data while filling in values in those with less than 70% using the impute R package. To ensure a consistent background, we analyzed only the 377,714 loci common to all three datasets. Samples with missing and zero survival time were deleted. For TCGA-SKCM dataset, gene expression and mutation data were also download for further validation analysis.

Identification of prognosis-related methylation loci pairs based on relative methylation orderings and construction of the risk predictive model

The methodology for developing a risk prognostic model using TCGA-SCKM methylation data as the training set is outlined as follows:

Identification of prognosis-related methylation loci pairs

We employed univariate Cox regression analysis to identify significant methylation loci with false discovery rate (FDR) of less than 0.1%, designating them as prognosis-related loci. These prognosis-related loci were formed into pairs, and the within-sample RMOs of the two loci in each pair was calculated according to Equation 1.

$$RMO(i, j) = \begin{cases} 1 & \text{if } \beta_i > \beta_j \\ 0 & \text{if } \beta_i \leq \beta_j \end{cases} \quad (1)$$

Here, β_i and β_j represent the methylation levels of locus i and j in a loci pair within a given sample.

The training samples were divided into two groups according to their RMO values for each pair of methylation loci: one group for samples with an RMO value of 1 and another for those with an RMO value of 0. Then, we used the log-rank test to evaluate overall survival (OS)

differences between the two groups. A pair was considered a prognostic methylation loci pair (PMLP) if the FDR-adjusted $p < 0.1\%$. The Cox proportional hazard model was used to compute the concordance index (C-index) value and the hazard ratio (HR). If a PMLP (i, j) had an RMO value of 1 and an HR value less than 1, it was adjusted to PMLP (j, i).

Identification of prognosis-related methylation loci pair combination using greedy algorithm

To identify the combination of PMLPs with the highest predictive efficacy, we implemented a greedy algorithm following these steps:

(1) Step 1: Initialization

We began by selecting the loci pair with the highest C-index value from the set of screened m PMLPs. This pair was designated as the initial combination, referred to as PairSet. The number of PMLPs n in PairSet was initialized to 1.

(2) Step 2: Iterative optimization

We then conducted the following operations among the remaining $m-n$ PMLPs. First, each remaining PMLP was selected sequentially and added to the PairSet. After addition, update the value of n , and calculate the total RMO score of the entire combination across all samples after its inclusion. Here, the total RMO score is calculated by summing the values of RMOs of all n PMLPs in the combination (Equation 2). According to whether the total RMO score exceeded $1/2n$, we divided all training samples into two groups. Univariate Cox regression analysis was used to calculate the C-index of the combination. For each added PMLPs, the one that resulted in the highest C-index value was selected, and the PairSet was updated accordingly.

$$RMO\ score = \sum_{k=1}^n RMO_k \quad (2)$$

(3) Step 3: Convergence judgment

We repeated the operations outlined in Step 2 until no further increases in the C-index could

be achieved by adding a new PMLP to the combination.

Establishment of prognostic model

Calculate the RMO score for the final PMLP combination in each sample. According to Equation 2, the total RMO scores for the final combination can range from 0 to the number of pairs in the combination. Then, we assessed the OS differences between the two groups classified by each RMO score value. The RMO score that demonstrated the most significant OS difference was selected as the risk threshold for prediction.

Assessment of the predictive performance of the prognostic model

The sensitivity and specificity of the prognostic model were assessed by using the time-dependent receiver operating characteristic (ROC) curve to calculate the area under the curve (AUC) at 1, 3, and 5 years. Multivariate Cox regression analyses were used to explore the independence of the prognostic model from other clinical factors, such as gender, age, and stage.

Immune infiltration analysis

We used the EpiDISH R package to evaluate the infiltration levels of seven immune cell types in SKCM samples [16] and calculated the Pearson correlation coefficients between the methylation levels of loci in the prognostic model and the infiltration levels of immune cells.

Enrichment analysis

The ChAMP R package was used for differential analysis between high- and low-risk groups [17]. Methylation loci satisfying $FDR < 5\%$ and $|\Delta\beta| > 0.1$ were identified as differentially methylated loci (DML). Based on the Gene Ontology (GO) and Kyoto Encyclopedia of Genes and Genomes (KEGG) databases, we used the gometh function from the missMethylR package to analyze the biological processes and pathways associated with the genes corresponding to DML [18,19].

Analysis of immunotherapy effect and chemotherapeutic drug sensitivity

In this study, we used the expression data for the training SKCM samples to assess the differences in immunotherapy efficacy and chemotherapeutic drug sensitivity between high- and low-risk groups.

To predict the patients' response to tumor immunogenicity, immunophenoscore (IPS) data of SKCM patients were downloaded from the TCIA database (<https://tcia.at/>). IPS was calculated by analyzing the gene expression Z-scores of specific cell types, such as activated CD4+ T cells, CD8+ T cells, and regulatory T cells. A higher IPS indicates increased immunogenicity [20]. Subsequently, all patients were divided into four groups according to the statuses of PD-1 or CTLA-4 (positive or negative). Finally, in each group, the Wilcoxon test was used to compare the IPS differences between the high- and low-risk groups.

Based on the Genomics of Drug Sensitivity in Cancer (GDSC) database, we used the oncoPredict R package to predict the response to commonly used chemotherapeutic drugs in SKCM [21,22]. The chemotherapy sensitivity of each tumor sample was evaluated using the half-maximal inhibitory concentration (IC50) value, with a lower IC50 value indicating higher sensitivity to the drug. The Wilcoxon test was used to compare the IC50 differences between the high- and low-risk groups.

Mutation characterization

We used the mutation profiles for the training SKCM samples to calculate the tumor mutational burden (TMB) of each sample, based on the total number of somatic base substitutions. Then, the Wilcoxon test was used to compare the TMB between high- and low-risk groups.

Performance comparison with other models

We collected six published prognostic models (Supplementary Table S2) constructed using TCGA-SKCM methylation data and compared

their predictive efficacy to our models in the validation datasets GSE51547 and GSE144487.

Statistical analysis

The data analysis in this study was mainly performed using R (version 4.3.1).

Results

Identification of prognostic methylation loci pair combination for skin cutaneous melanoma based on relative methylation orderings

To identify SKCM prognostic biomarkers, we used the DNA methylation profiles from 458 SKCM cases as the training set (Table 1). At first, we screened the CpG loci associated with SKCM prognosis using univariate Cox regression analysis. The results showed that 826 prognosis-related loci were significantly associated with OS at FDR < 0.1%. We generated 340,725 loci pairs by pairing these prognosis-related loci. Of these pairs 36,347 showed a statistically significant association with OS based on univariate Cox regression analysis, with FDR < 0.1%. We referred to these pairs as PMLPs for subsequent analyses.

Next, using these 36,347 PMLPs, we employed a greedy algorithm to find the optimal combination for SKCM, as described in the Methods section. The initial combination was selected based on the pair (cg02482460, cg04502490) with the highest C-index. The final combination, consisting of eight PMLPs, achieved the highest C-index value of 0.728 and was referred to as SKCM-P8. Details of the eight pairs of loci are provided in Supplementary Table S1. For SKCM-P8, the most significant OS difference between samples was observed at an RMO score of 3, which we designated as the threshold to predict risk groups in subsequent analyses.

In the training set, 304 and 154 samples were divided into high- and low-risk groups by SKCM-P8, respectively. Kaplan–Meier survival analysis showed that there was a significant difference in OS, with a significant decrease in the survival of patients in the high-risk group (log-rank test, $p < 0.0001$, HR = 0.26, 95% CI: 0.18–0.36, Figure 1a). ROC curves showed AUCs of 0.81, 0.83, and 0.84 for 1, 3, and 5 years, survival, respectively

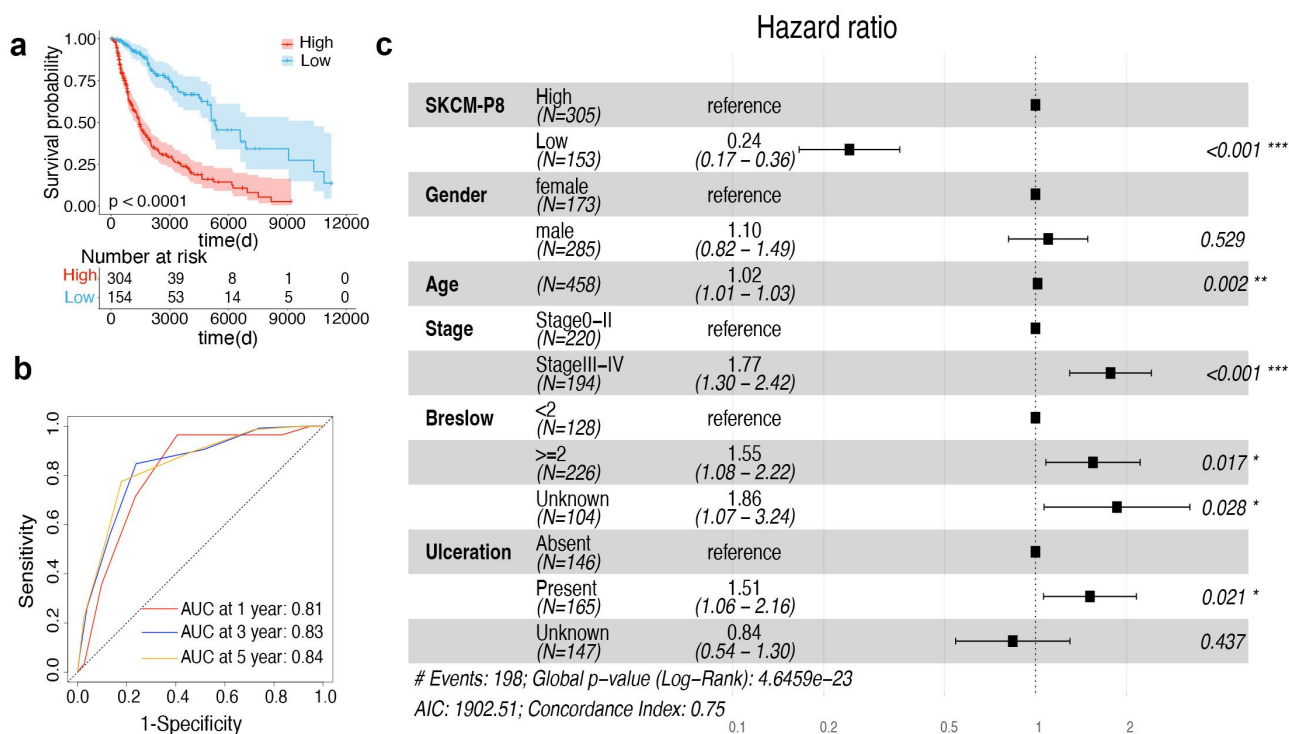


Figure 1. Survival analysis results of SKCM-P8 in the training set. (a) Kaplan-Meier survival plots for the high- and low-risk groups based on SKCM-P8; (b) time-dependent ROC curves for SKCM-P8 predicting OS at 1, 3, and 5 years; (c) forest plots displaying the results of multivariate Cox regression analysis. Statistical significance is indicated by asterisks: * $p < 0.05$, ** $p < 0.01$, *** $p < 0.001$.

(Figure 1b). Multifactorial Cox regression analyses showed that SKCM-P8 could be an independent prognostic indicator after adjusting for clinical characteristics such as gender, age, stage, and the presence or absence of ulcers and Breslow thickness ($p < 0.001$, Figure 1c). These results suggest that SKCM-P8 has strong predictive performance for the prognosis of SKCM.

Validation of SKCM-P8 in independent datasets

We further validated the prognostic prediction performance of SKCM-P8 in two independent datasets. In GSE51547, 32 and 15 samples were classified into high- and low-risk groups, while in GSE144487, 109 and 85 were stratified into high- and low-risk samples, respectively. Kaplan–Meier survival analyses showed that in both datasets, the high-risk group had significantly lower OS rates ($p = 0.017$, HR = 0.44, 95% CI: 0.22–0.87, Figure 2a; $p = 0.00028$, HR = 0.51, 95% CI: 0.35–0.74, Figure 2b). Time-dependent ROC curves showed AUC values of

0.75, 0.77, 0.87 in GSE51547 (Figure 2c) and 0.57, 0.65, 0.61 in GSE144487 (Figure 2d) for 1, 3 and 5 years OS, respectively. Multifactorial Cox regression analyses showed that SKCM-P8 served as an independent prognostic factor for SKCM, independent of gender, subtype, Breslow thickness, and stage ($p < 0.05$, Figure 2e,f). These findings indicate that the performance of SKCM-P8 is reproducible across datasets.

Functional enrichment analysis of differentially methylated loci between high- and low-risk patients stratified by SKCM-P8

In the training set, we detected 8,011 DML between the high- and low-risk patients stratified by SKCM-P8, with FDR < 5% and $|\Delta\beta| > 0.1$. Functional enrichment analysis of these DML revealed that the associated genes were mainly enriched in the GO database for biological processes such as T cell activation, regulation of leukocyte activation, and facilitation of the

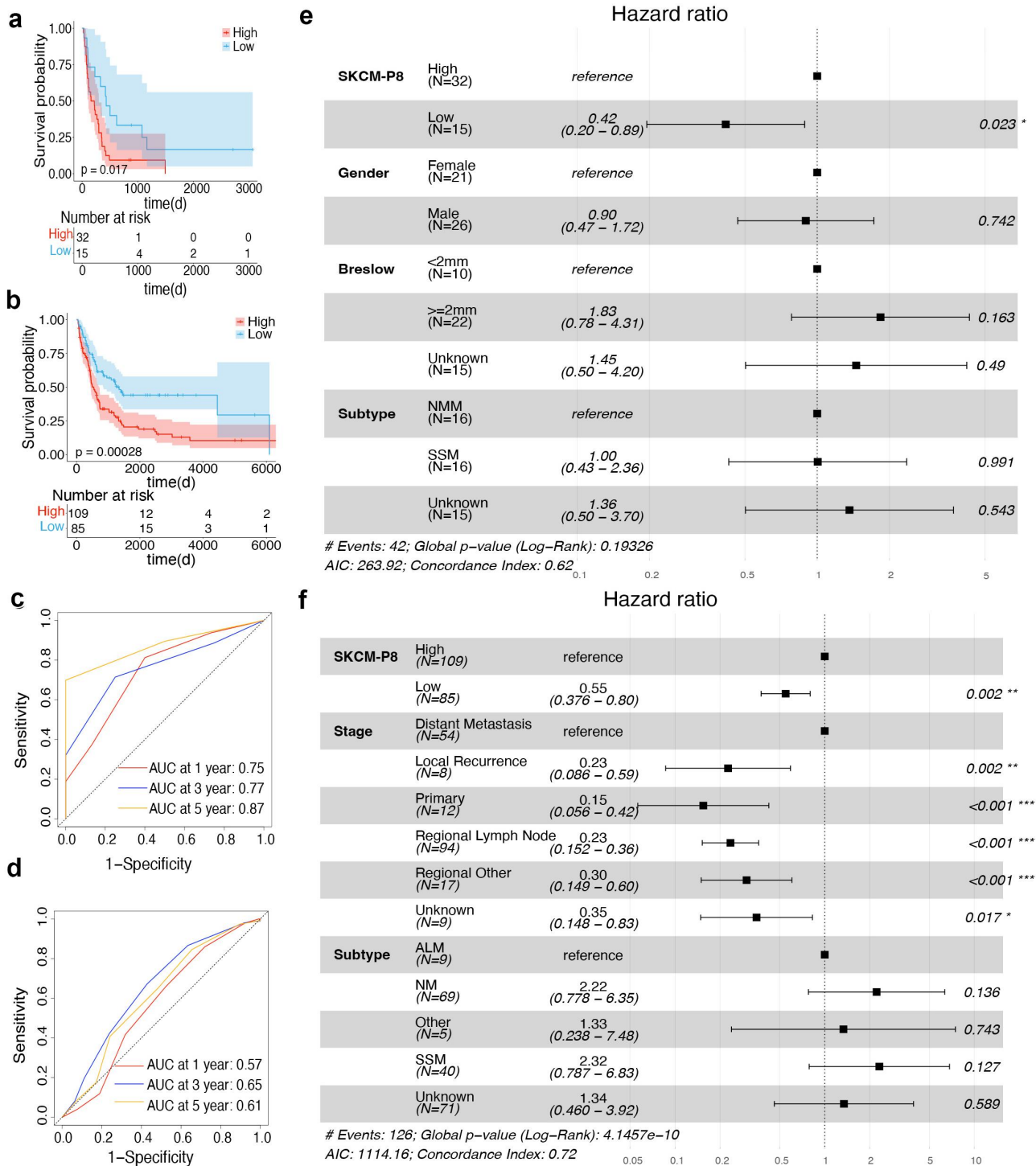


Figure 2. Predictive efficacy of SKCM-P8 in two validation datasets. (a-b) Kaplan-Meier survival plots for high- and low-risk groups in GSE15147 (a) and GSE14487 (b); (c-d) time-dependent ROC curves of SKCM-P8 predicting OS at 1, 3, and 5 years in GSE15147 (c) and GSE14487 (d); (e-f) forest plots displaying the results of multivariate Cox regression analyses for GSE15147 (e) and GSE14487 (f). Statistical significance is indicated by asterisks: * $p < 0.05$, ** $p < 0.01$, *** $p < 0.001$.

positive regulation of immune system processes (Figure 3a). In the KEGG database, the enriched pathways included the Notch signaling pathway, Rap1 signaling pathway, ERBB signaling

pathway and other pathways (Figure 3b). The findings in functional analysis suggested that SKCM-P8 May play role in immune system regulation.

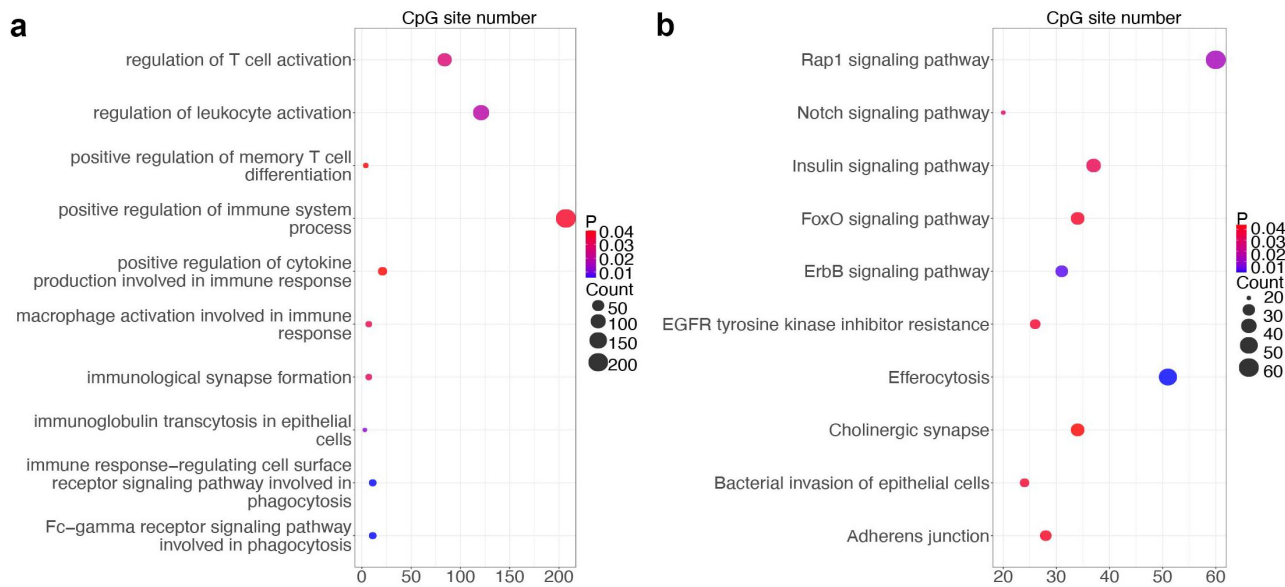


Figure 3. Functional enrichment analysis of DML. (a) Important GO processes enriched by DML; (b) important KEGG pathways enriched by DML.

Immune system association of SKCM-P8 through immune infiltration analysis

To further explore the association between SKCM-P8 and the immune system, we conducted an immune infiltration analysis. In the training set, patients in the low-risk group had higher levels of CD8+ T cells and B cells, while those in the high-risk group had higher levels of monocytes

($p < 0.05$, Figure 4a). This finding suggests that the patients in the low-risk group may have stronger immune responses. When analyzing the 16 loci in the SKCM-P8, we found that all loci showed significantly differential methylation levels between the high- and low-risk groups (Figure 4b). Correlation analysis further revealed that some loci were negatively correlated with CD8+ T cells, B lymphocytes, and CD4+ T cells, while the other were positively correlated with T and B lymphocytes (Figure 4c). These results suggest that SKCM-P8 can reflect prognosis-related immune information.

Correlation of risk groupings with tumor mutations

Our analysis revealed a significantly higher TMB in the low-risk group compared to the high-risk group in the training dataset (Wilcoxon test, $p <$

0.05, Figure 4d). Considering that TMB is a crucial indicator of neoantigen production by tumors, patients in the low-risk group may benefit from treatment with immune checkpoint inhibitors.

Differential responses to chemotherapy and immunotherapy in patients stratified by SKCM-P8

To evaluate whether there is a difference in immunotherapy between the two groups classified by SKCM-P8, we predicted the IC50 values of commonly used chemotherapy drugs using gene expression data from SKCM patients. The results showed that, in the training dataset, patients in the low-risk group exhibited lower IC50 values, indicating a higher sensitivity to chemotherapy compared to the high-risk individuals (Wilcoxon test, $p < 0.05$, Figure 5a–h).

We further examined the IPS data for SKCM to compare immunotherapy response between the high- and low-risk groups. The analysis revealed that IPS was generally higher in the low-risk group of patients (Wilcoxon test, $p < 0.05$, Figure 5i–l), either alone or in combination of anti-CTLA-4 and anti-PD-1 therapy, suggesting more beneficial for patients in the low-risk group.

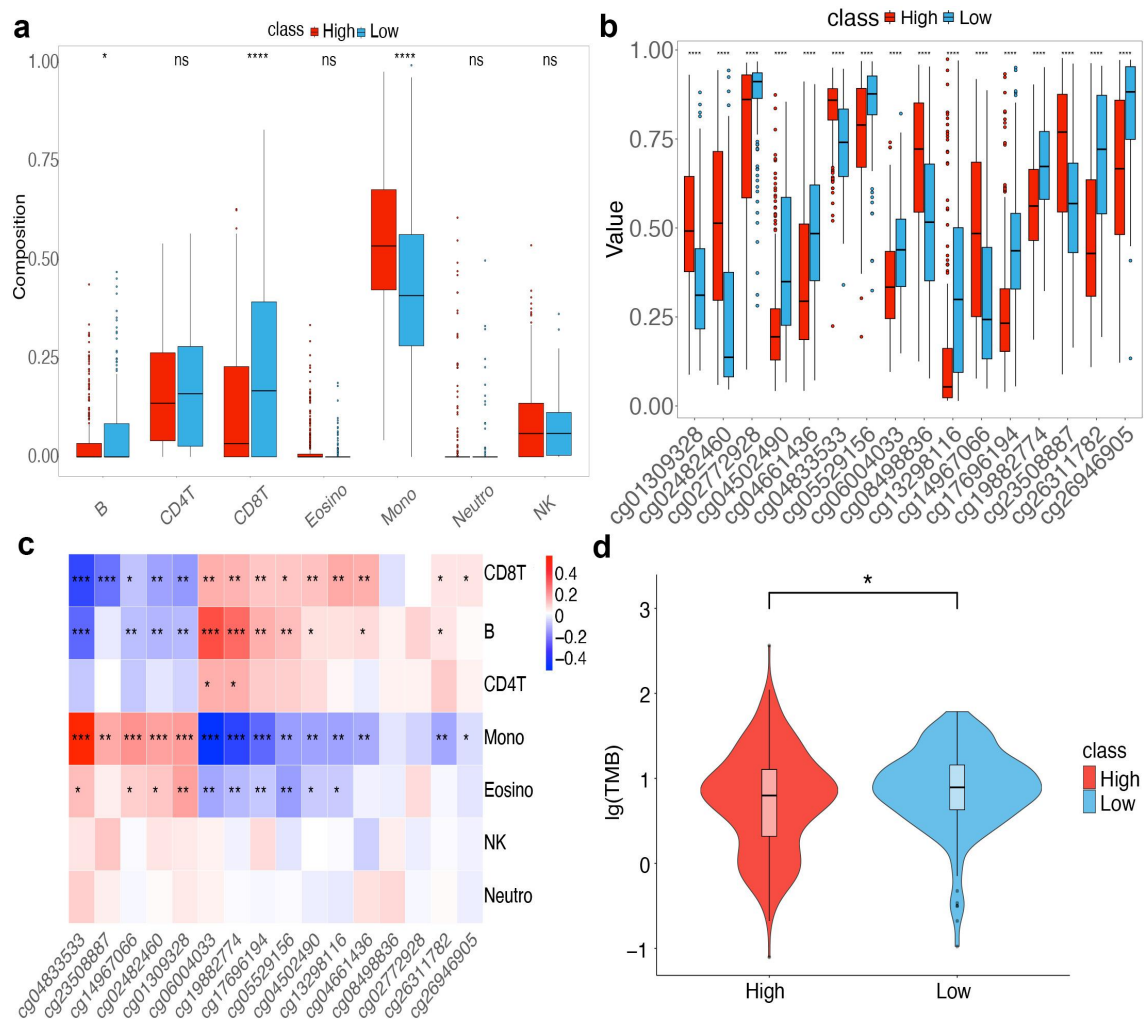


Figure 4. Immune cell infiltration, differential methylation levels of 16 loci in SKCM-P8 and their correlation with immune cell types, and tumor mutational burden analysis between high- and low-risk groups. (a) Immune cell composition in training SKCM samples. (b) Box plots showing the differential methylation levels of the 16 loci in SKCM-P8 between high- and low-risk groups. (c) Correlation matrix illustrating the relationships between the 16 loci in SKCM-P8 and various immune cell types. (d) Comparison of tumor mutational burden between high and low-risk groups. Statistical significance levels are indicated by asterisks: ns, not significant ($p > 0.05$), * $p < 0.05$, ** $p < 0.01$, *** $p < 0.001$, **** $p < 0.0001$.

The above findings highlight significant differences in the responses to both chemotherapy and immunotherapy based on risk stratification, suggesting that SKCM-P8 could be a valuable reference for tailoring follow-up treatment strategies for SKCM patients.

Comparison the prognostic predictive efficacy of SKCM-P8 with published models

We collected six published prognostic models established using TCGA-SKCM methylation data (detailed in Supplementary Table S2) and

evaluated their prognostic performance in the two validation datasets we used.

In the GSE51547 dataset, we analyzed all six models and found that only Model 2 exhibited a statistically significant difference in OS between its predicted high- and low-risk groups ($p = 0.0022$, HR = 0.35, 95% CI: 0.17–0.70, Figure 6a). Specifically, the OS of the high-risk group was significantly lower than that of the low-risk group, consistent with the results of SKCM-P8 (Figure 1a).

In GSE144487, due to the undetected methylation loci in Model 6, we only evaluated five prognostic models. The results showed that only Model 1 and

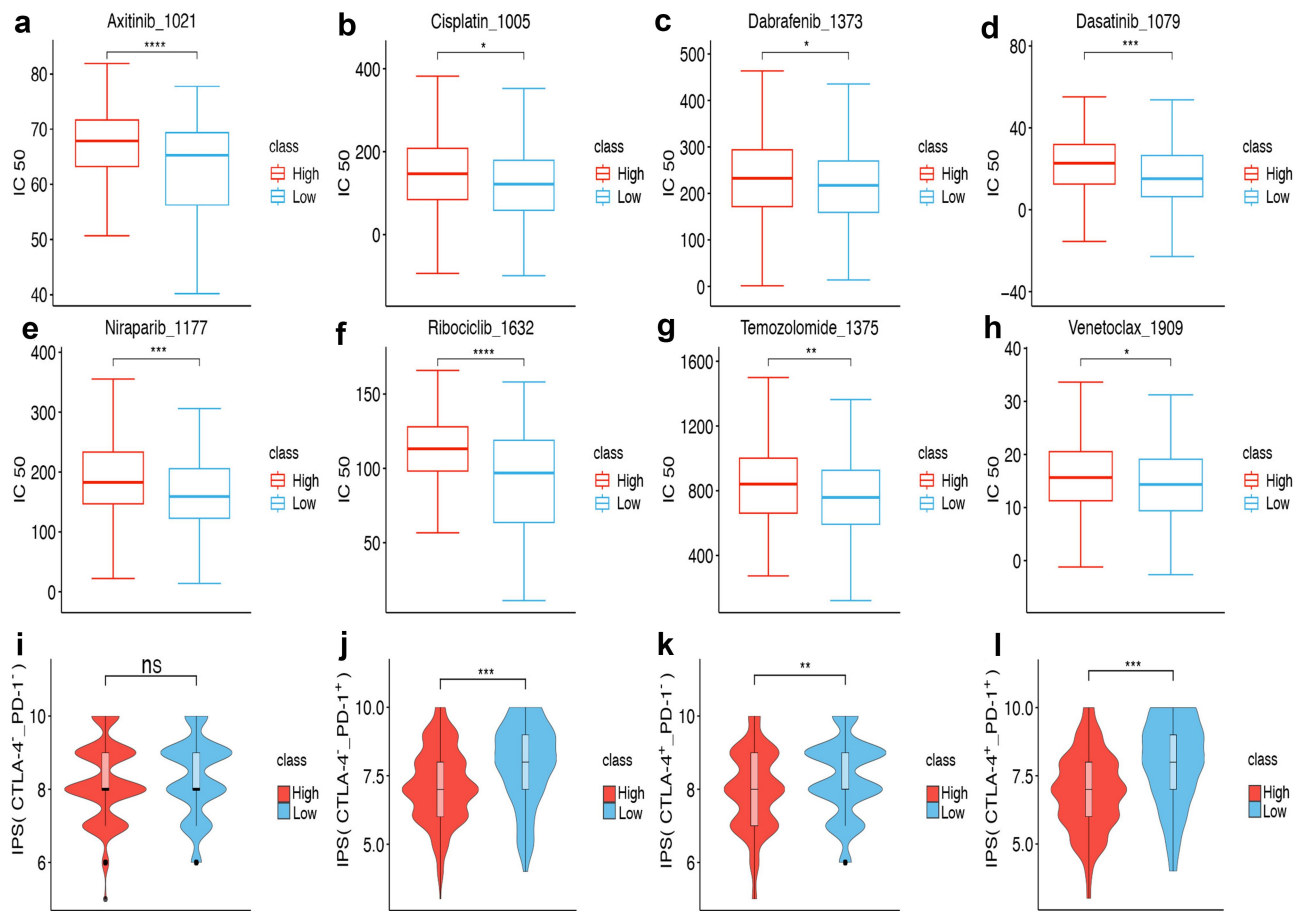


Figure 5. Drug sensitivity analysis between high- and low-risk groups. (a-h) Differences in IC₅₀ of various chemotherapy drugs between high- and low-risk groups; (i-l) differences in IPS stratified by PD-1 and CTLA-4 expression status (e.g., “CTLA-4⁺PD-1⁺” indicates CTLA-4-positive and PD-1-negative responses). Statistical significance was determined by the Wilcoxon test: ns, not significant ($p > 0.05$), * $p < 0.05$, ** $p < 0.01$, *** $p < 0.001$, **** $p < 0.0001$.

Model 3 were able to classify risk groups with a statistically significant difference in OS (Model 1: $p = 0.0022$, HR = 0.46, 95% CI: 0.30–0.70; Model 3: $p = 0.018$, HR = 0.65, 95% CI: 0.46–0.93, Figure 6b). Both models indicated that the OS of the high-risk group was lower than that of the low-risk group, although the magnitude and significance of the difference varied, further validating the predictive result of SKCM-P8 (Figure 1a).

Notably, when comparing the C-index of these models, we found that our SKCM-P8 model exhibited a higher C-index value in both datasets, particularly in the GSE144487 dataset, where its C-index reached 0.656 (Figure 6c).

The above results indicate that, compared to the other evaluated models, SKCM-P8 demonstrated good robustness and prediction performance in two independent datasets.

Discussion

SKCM as an extremely aggressive cancer, has been a clinical challenge with its high metastasis and poor prognosis [23]. In this study, we successfully developed a prognostic model, SKCM-P8, based on the RMOs of methylation loci. This model demonstrated robust predictive ability in independent datasets, offering a valuable reference for personalized treatment options in SKCM patients.

Our KEGG enrichment analysis revealed that the DML between high- and low-risk groups were enriched in SKCM-related signaling pathways, such as Rap1 and Notch. The Rap1 signaling pathway regulates cell migration and polarization, which is critical for tumor metastasis [24]. This finding aligns with previous SKCM prognostic studies, where prognostic genes were commonly enriched in the Rap1 signaling pathway [25–27].

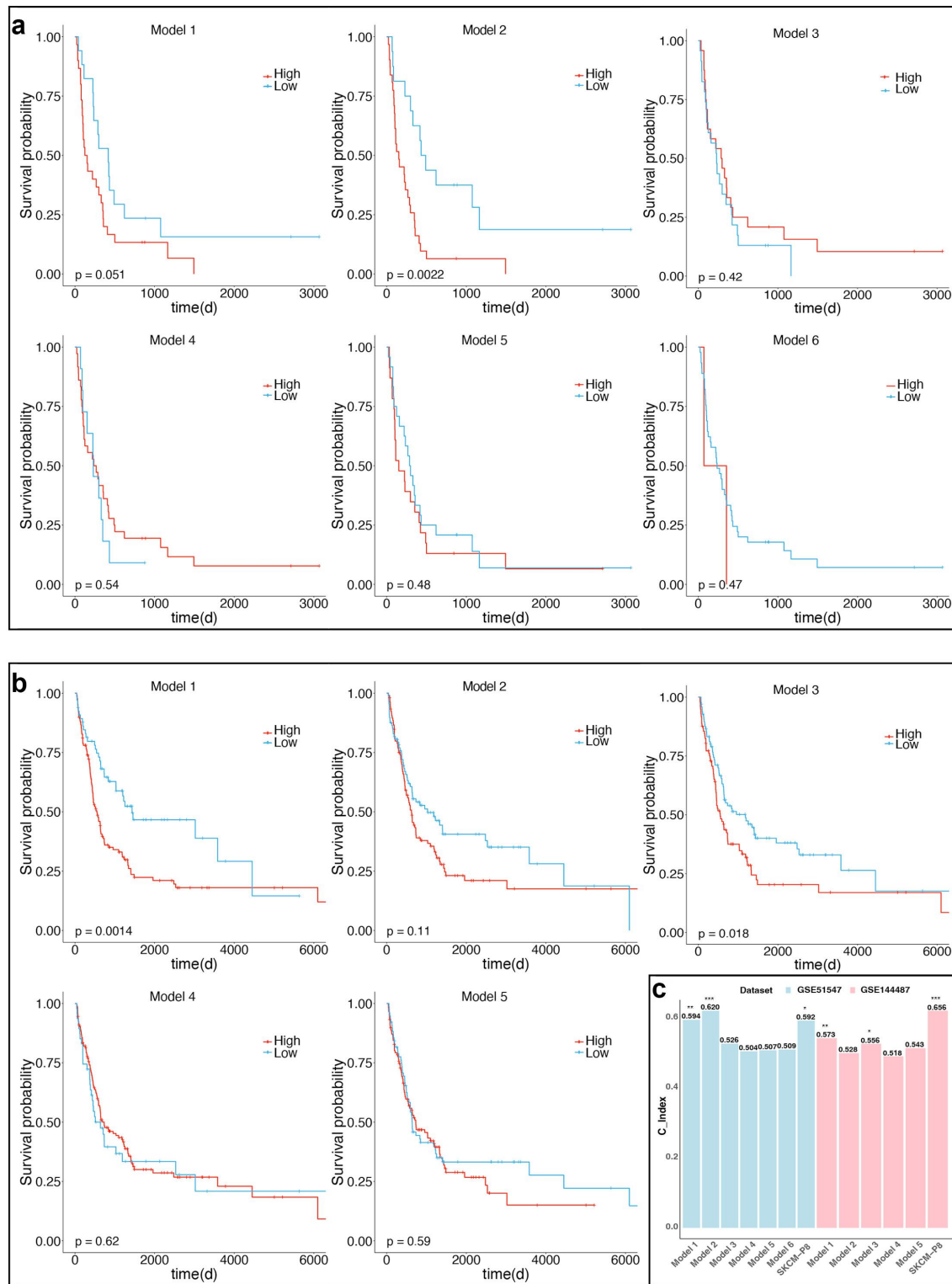


Figure 6. Kaplan-Meier survival plots for six published models and C-index comparison to SKCM-P8. (a) Kaplan-Meier survival plots for six published models in GSE51547; (b) Kaplan-Meier survival plots for five published models in GSE144487; (c) histogram comparing the C-index values of the six published models and SKCM-P8. The top three models, including SKCM-P8, are marked with decreasing asterisks (***, **, *), indicating their relative performance based on the C-index values.

The Notch signaling pathway is an evolutionarily conserved inter-cellular signaling cascade response that has been shown to promote tumor growth in SKCM [28]. Multiple studies have found that SKCM cells depend on Notch1 signaling to maintain growth and survival [29–31]. Therefore, modulation of the Notch1 pathway has important therapeutic potential, and several inhibition strategies targeting the Notch pathway have been used to treat SKCM and other cancers [32]. Additionally, studies have shown that Notch and ERBB signaling pathway components are concurrently dysregulated in SKCM, and it is speculated that the growth and progression of SKCM may depend on the combined action of these two signaling pathways [33].

Our analysis of the high- and low-risk groups divided by SKCM-P8 revealed significant differences in immune cell infiltration, drug sensitivity, and TMB. Notably, patients in high-risk group exhibited lower immune cell content, suggesting a potential association between immune cell imbalance and poor prognosis [34]. This findings aligns with a research indicating increased myeloid components (such as neutrophils and monocytes) and decreased lymphoid components during disease metastasis [35]. In particular, higher monocyte counts were associated with poor prognosis in stage IV SKCM patients [35]. Furthermore, we observed significant differences in TMB between the high- and low-risk groups, with the low-risk samples having higher mutational loads. Previous studies have shown that tumors with high mutational loads tend to respond better to checkpoint blockade-based immunotherapy, indicating potential therapeutic implications for low-risk patients [36,37]. Additionally, our drug sensitivity analyses further confirmed that high-risk patients exhibited lower sensitivity to both chemotherapy and immune checkpoint inhibitors, potentially predict poorer survival outcomes.

As an exploratory analysis, at the transcriptome level, we analyzed the expression differences of the 21 genes corresponding to the methylation loci in SKCM-P8 using TCGA-SKCM RNA-seq data. Notably, 12 of these genes showed significant differences in expression between high- and low-risk

groups ($p < 0.05$, Supplementary Fig.S1), and 11 were significantly associated with OS in SKCM (univariate Cox regression analysis, $p < 0.05$, Supplementary Table S3). Notably, nine genes were both significantly differential expressed between high- and low-risk groups and significantly associated with OS. Among them, *PSMB8* and *PSMB9* are two major components of the immunoproteasome subunit. It has been suggested that their expression levels may serve as prognostic markers of survival in SKCM patients, and may help identify patients who may respond better to immune checkpoint inhibitors [38]. Moreover, the expression of *GBP* has been associated with the prognosis of several cancers [39] and *IFITM1* has been suggested to be associated with the prognosis of SKCM [40].

Expanding on pathway interactions, we screened 1,601 loci exhibiting significant correlations with those in SKCM-P8 (Pearson's correlation coefficient $r > 0.7$, $p < 0.05$). KEGG pathway enrichment analysis revealed that these loci were predominantly enriched in immune-related pathways, including TNF signaling, Th17 cell differentiation, T cell receptor signaling, and Transforming Growth Factor-beta ($TGF-\beta$) signaling pathway, with the PD-L1 expression and PD-1 checkpoint pathway in cancer emerging as the top enriched pathway (Supplementary Fig.S2). Strikingly, the PD-1/PD-L1 pathway is a critical immune checkpoint pathway that controls the induction and maintenance of immune tolerance within the tumor microenvironment. The activity of PD-1 and its ligands PD-L1 or PD-L2 are responsible for T cell activation, proliferation, and cytotoxic secretion in cancer to degenerating anti-tumor immune responses [41]. $TGF-\beta$ is a classic membrane-to-nucleus signaling cascade closely related to immune regulation. In melanoma, $TGF-\beta$ promotes immune evasion by upregulating Indoleamine 2,3-dioxygenase and C-C Motif Ligand 22 in dendritic cells, increasing regulatory T cell infiltration, and suppressing anti-tumor immunity [42]. Its critical role in tumor progression has spurred clinical interest, with $TGF-\beta$ inhibitors now under development to enhance immunotherapy responses [43]. These findings solidify SKCM-P8's connection to immune microenvironment, providing mechanistic for its clinical utility in guiding immunotherapy.

To further dissect immune interactions, we analyzed correlations between SKCM-P8 methylation loci and immune checkpoint expression. The methylation loci in SKCM-P8 showed bidirectional correlations with immune checkpoints. For example, locus cg04833533 correlated negatively and cg06004033 positively with all immune checkpoints (Supplementary Fig.S3). These bidirectional relationships suggest SKCM-P8's epigenetic regulation of immune checkpoints may shape the tumor-immune landscape, underscoring its prognostic relevance.

This study is a retrospective study and lacks prospective clinical data support. To further validate the predictive effect of SKCM-P8, future research should incorporate prospective cohort studies involving larger sample sizes and diverse patient populations. Additionally, it would be beneficial to gather detailed clinical outcomes, treatment responses, and follow-up data to establish a clearer correlation between the predictive biomarkers identified in SKCM-P8 and patient prognosis.

Conclusion

In conclusion, SKCM-P8 is a reliable and robust qualitative biomarker that stratifies SKCM patients into high- and low-risk categories, offering potential for personalized clinical applications. By reflecting immune information and predicting treatment responses, SKCM-P8 emerges as a promising tool for guiding therapeutic decisions in the management of SKCM.

Disclosure statement

No potential conflict of interest was reported by the author(s).

Funding

The work was supported by the Thousand Talents Program of Jiangxi for High-level talents in innovation and entrepreneurship [Jxsq2020101096].

Authors' contributions

HDL and **GNH** conceived the idea and conceptualized the study. **YH** and **HDL** conducted the bioinformatics analysis and interpreted the results. **YRG** and **JYR** collected and

preprocessed data. **YH** and **LLW** generated the figures and tables. **YH** and **HDL** wrote the paper. **GNH** supervised the whole study process. **HDL** and **GNH** revised the manuscript. All authors have read and approved the final version of the manuscript.

Data availability statement

The datasets analyzed during the current study are available in TCGA (<https://www.cancer.gov/ccg/research/genome-sequencing/tcga>), and GEO (<https://www.ncbi.nlm.nih.gov/>) with accession numbers GSE51547 and GSE144487.

Abbreviations

SKCM	Skin cutaneous melanoma
TCGA	The Cancer Genome Atlas
RMOs	relative methylation orderings
GEO	Gene Expression Omnibus
FDR	false discovery rate
OS	overall survival
PMLP	prognostic methylation loci pair
C-index	concordance index
HR	hazard ratio
ROC	receiver operating characteristic
AUC	area under the curve
DML	differentially methylated loci
GO	Gene Ontology
KEGG	Kyoto Encyclopedia of Genes and Genomes
IPS	immunophenoscore
GDSC	Genomics of Drug Sensitivity
IC50	half-maximal inhibitory concentration
TMB	tumor mutational burden.

ORCID

Guini Hong  <http://orcid.org/0000-0002-0277-6123>

References

- [1] Zhu Y, Han D, Duan H, et al. Identification of pyroptosis-relevant signature in tumor immune micro-environment and prognosis in skin cutaneous melanoma using network analysis. *Stem Cells Int.* 2023;2023:1–39. doi: [10.1155/2023/3827999](https://doi.org/10.1155/2023/3827999)
- [2] Hyams DM, Cook RW, Buzaid AC. Identification of risk in cutaneous melanoma patients: prognostic and predictive markers. *J Surg Oncol.* 2019;119(2):175–186. doi: [10.1002/jso.25319](https://doi.org/10.1002/jso.25319)
- [3] Deng J, Lin J, Liu C, et al. N7-methylguanosine methylation-related regulator genes as biological markers in predicting prognosis for melanoma. *Sci Rep.* 2022;12(1):21082. doi: [10.1038/s41598-022-25698-x](https://doi.org/10.1038/s41598-022-25698-x)
- [4] Li HD, Hong GN, Guo Z. Age-related DNA methylation changes in peripheral whole blood. *Yi Chuan.* 2015;37(2):165–173. doi: [10.16288/j.yczz.14-394](https://doi.org/10.16288/j.yczz.14-394)

- [5] Urbano A, Smith J, Weeks RJ, et al. Gene-specific targeting of DNA methylation in the mammalian genome. *Cancers (Basel)*. 2019;11(10):11. doi: [10.3390/cancers11101515](https://doi.org/10.3390/cancers11101515)
- [6] Roh MR, Gupta S, Park KH, et al. Promoter methylation of PTEN is a significant prognostic factor in melanoma survival. *J Invest Dermatol*. 2016;136(5):1002–1011. doi: [10.1016/j.jid.2016.01.024](https://doi.org/10.1016/j.jid.2016.01.024)
- [7] Micevic G, Thakral D, McGearry M, et al. PD-L1 methylation regulates PD-L1 expression and is associated with melanoma survival. *Pigment Cell Melanoma Res*. 2019;32(3):435–440. doi: [10.1111/pcmr.12745](https://doi.org/10.1111/pcmr.12745)
- [8] Marzese DM, Scolyer RA, Huynh JL, et al. Epigenome-wide DNA methylation landscape of melanoma progression to brain metastasis reveals aberrations on homeobox D cluster associated with prognosis. *Hum Mol Genet*. 2014;23:226–238.
- [9] Guo W, Zhu L, Zhu R, et al. A four-DNA methylation biomarker is a superior predictor of survival of patients with cutaneous melanoma. *Elife*. 2019;8. doi: [10.7554/eLife.44310](https://doi.org/10.7554/eLife.44310)
- [10] Tengda L, Cheng Q, Yi S. Identification of melanoma subsets based on DNA methylation sites and construction of a prognosis evaluation model. *J Oncol*. 2022;2022:6608650.
- [11] Ralser DJ, Herr E, de Vos L, et al. ICOS DNA methylation regulates melanoma cell-intrinsic ICOS expression, is associated with melanoma differentiation, prognosis, and predicts response to immune checkpoint blockade. *Biomark Res*. 2023;11(1):56. doi: [10.1186/s40364-023-00508-2](https://doi.org/10.1186/s40364-023-00508-2)
- [12] Li H, Hong G, Xu H, et al. Application of the rank-based method to DNA methylation for cancer diagnosis. *Gene*. 2015;555(2):203–207. doi: [10.1016/j.gene.2014.11.004](https://doi.org/10.1016/j.gene.2014.11.004)
- [13] Zeng L, Li K, Wei H, et al. Signature consist of nine differentially methylated gene pairs to predict the prognosis for stage II colorectal cancer patients. *Oncotarget*. 2018;0(0). doi: [10.18632/oncotarget.23979](https://doi.org/10.18632/oncotarget.23979)
- [14] Ge F, Zhang P, Niu J, et al. NDRG2 and TLR7 as novel DNA methylation prognostic signatures for acute myelocytic leukemia. *J Cell Physiol*. 2020;235(4):3790–3797. doi: [10.1002/jcp.29273](https://doi.org/10.1002/jcp.29273)
- [15] Wei Z, Wu B, Wang L, et al. A large-scale transcriptome analysis identified ELANE and PRTN3 as novel methylation prognostic signatures for clear cell renal cell carcinoma. *J Cell Physiol*. 2020;235(3):2582–2589. doi: [10.1002/jcp.29162](https://doi.org/10.1002/jcp.29162)
- [16] Zheng SC, Breeze CE, Beck S, et al. EpiDISH web server: epigenetic dissection of intra-sample-heterogeneity with online GUI. *Bioinformatics*. 2019;36(6):1950–1951. doi: [10.1093/bioinformatics/btz833](https://doi.org/10.1093/bioinformatics/btz833)
- [17] Morris TJ, Butcher LM, Feber A, et al. ChAMP: 450k chip analysis methylation pipeline. *Bioinformatics*. 2014;30(3):428–430. doi: [10.1093/bioinformatics/btt684](https://doi.org/10.1093/bioinformatics/btt684)
- [18] Maksimovic J, Oshlack A, Phipson B. Gene set enrichment analysis for genome-wide DNA methylation data. *Genome Biol*. 2021;22(1):173. doi: [10.1186/s13059-021-02388-x](https://doi.org/10.1186/s13059-021-02388-x)
- [19] Phipson B, Maksimovic J, Oshlack A. missMethyl: an R package for analyzing data from Illumina's HumanMethylation450 platform. *Bioinformatics*. 2016;32:286–288.
- [20] Mei J, Xing Y, Lv J, et al. Construction of an immune-related gene signature for prediction of prognosis in patients with cervical cancer. *Int Immunopharmacol*. 2020;88:106882. doi: [10.1016/j.intimp.2020.106882](https://doi.org/10.1016/j.intimp.2020.106882)
- [21] Yang W, Soares J, Greninger P, et al. Genomics of drug sensitivity in cancer (GDSC): a resource for therapeutic biomarker discovery in cancer cells. *Nucleic Acids Res*. 2013;41(D1):D955–61. doi: [10.1093/nar/gks1111](https://doi.org/10.1093/nar/gks1111)
- [22] Maeser D, Gruener RF, Huang RS. oncoPredict: an R package for predicting in vivo or cancer patient drug response and biomarkers from cell line screening data. *Brief Bioinform*. 2021;22(6):22. doi: [10.1093/bib/bbab260](https://doi.org/10.1093/bib/bbab260)
- [23] Xue W, Zhu H, Liu H, et al. DIRAS2 is a prognostic biomarker and linked with immune infiltrates in melanoma. *Front Oncol*. 2022;12:799185. doi: [10.3389/fonc.2022.799185](https://doi.org/10.3389/fonc.2022.799185)
- [24] Zhang YL, Wang RC, Cheng K, et al. Roles of Rap1 signaling in tumor cell migration and invasion. *Cancer Biol Med*. 2017;14(1):90–99. doi: [10.20892/j.issn.2095-3941.2016.0086](https://doi.org/10.20892/j.issn.2095-3941.2016.0086)
- [25] Liu C, Liu Y, Yu Y, et al. Comprehensive analysis of ferroptosis-related genes and prognosis of cutaneous melanoma. *BMC Med Genomics*. 2022;15(1):39. doi: [10.1186/s12920-022-01194-z](https://doi.org/10.1186/s12920-022-01194-z)
- [26] Kutlay A, Aydin Son Y. Integrative predictive modeling of metastasis in melanoma cancer based on MicroRNA, mRNA, and DNA methylation data. *Front Mol Biosci*. 2021;8:637355.
- [27] Han Y, Li X, Yan J, et al. Bioinformatic analysis identifies potential key genes in the pathogenesis of melanoma. *Front Oncol*. 2020;10:581985. doi: [10.3389/fonc.2020.581985](https://doi.org/10.3389/fonc.2020.581985)
- [28] Zhang W, Liu H, Liu Z, et al. Functional variants in notch pathway genes NCOR2, NCSTN, and MAML2 predict survival of patients with cutaneous melanoma. *Cancer Epidemiol Biomarkers Prev*. 2015;24(7):1101–1110. doi: [10.1158/1055-9965.EPI-14-1380-T](https://doi.org/10.1158/1055-9965.EPI-14-1380-T)
- [29] Zhang K, Wong P, Zhang L, et al. A Notch1-neuregulin1 autocrine signaling loop contributes to melanoma growth. *Oncogene*. 2012;31(43):4609–4618. doi: [10.1038/onc.2011.606](https://doi.org/10.1038/onc.2011.606)
- [30] Liu ZJ, Xiao M, Balint K, et al. Notch1 signaling promotes primary melanoma progression by activating mitogen-activated protein kinase/phosphatidylinositol 3-kinase-Akt pathways and up-regulating N-cadherin expression. *Cancer Res*. 2006;66:4182–4190.
- [31] Qiu H, Zmina PM, Huang AY, et al. Inhibiting Notch1 enhances immunotherapy efficacy in melanoma by preventing Notch1 dependent immune suppressive properties. *Cancer Lett*. 2018;434:144–151.
- [32] de Oliveira Filho RS, Soares AL, Paschoal FM, et al. Literature review of notch melanoma receptors. *Surg Exp Pathol*. 2019;2(1). doi: [10.1186/s42047-019-0052-9](https://doi.org/10.1186/s42047-019-0052-9)

- [33] Bedogni B. Notch signaling in melanoma: interacting pathways and stromal influences that enhance notch targeting. *Pigment Cell Melanoma Res.* 2014;27(2):162–168. doi: [10.1111/pcmr.12194](https://doi.org/10.1111/pcmr.12194)
- [34] Ali HR, Chlon L, Pharoah PD, et al. Patterns of immune infiltration in breast cancer and their clinical implications: a gene-expression-based retrospective study. *PLOS Med.* 2016;13(12):e1002194. doi: [10.1371/journal.pmed.1002194](https://doi.org/10.1371/journal.pmed.1002194)
- [35] Gandini S, Ferrucci PF, Botteri E, et al. Prognostic significance of hematological profiles in melanoma patients. *Int J Cancer.* 2016;139:1618–1625.
- [36] Van Allen EM, Miao D, Schilling B, et al. Genomic correlates of response to CTLA-4 blockade in metastatic melanoma. *Science.* 2015;350(6257):207–211. doi: [10.1126/science.aad0095](https://doi.org/10.1126/science.aad0095)
- [37] Rizvi NA, Hellmann MD, Snyder A, et al. Mutational landscape determines sensitivity to PD-1 blockade in non-small cell lung cancer. *Science.* 2015;348(6230):124–128. doi: [10.1126/science.aaa1348](https://doi.org/10.1126/science.aaa1348)
- [38] Kalaora S, Lee JS, Barnea E, et al. Immunoproteasome expression is associated with better prognosis and response to checkpoint therapies in melanoma. *Nat Commun.* 2020;11(1):896. doi: [10.1038/s41467-020-14639-9](https://doi.org/10.1038/s41467-020-14639-9)
- [39] Wang Q, Wang X, Liang Q, et al. Distinct prognostic value of mRNA expression of guanylate-binding protein genes in skin cutaneous melanoma. *Oncol Lett.* 2018;15:7914–7922.
- [40] He Z, Chen M, Luo Z. Identification of immune-related genes and integrated analysis of immune-cell infiltration in melanoma. *Aging (Albany NY).* 2024;16:911–927.
- [41] Han Y, Liu D, Li L. PD-1/PD-L1 pathway: current researches in cancer. *Am J Cancer Res.* 2020;10:727–742.
- [42] Hanks BA, Holtzhausen A, Evans KS, et al. Type III TGF- β receptor downregulation generates an immunotolerant tumor microenvironment. *J Clin Invest.* 2013;123(9):3925–3940. doi: [10.1172/JCI65745](https://doi.org/10.1172/JCI65745)
- [43] Zhao H, Wei J, Sun J. Roles of TGF- β signaling pathway in tumor microenvironment and cancer therapy. *Int Immunopharmacol.* 2020;89:107101. doi: [10.1016/j.intimp.2020.107101](https://doi.org/10.1016/j.intimp.2020.107101)